

# Liquid crystal elastomer and fabric bilayer actuators

Sophia Eristoff<sup>1</sup>, Lily Behnke<sup>1</sup>, Lina Sanchez-Botero<sup>1,†</sup>, Sree Kalyan Patiballa<sup>1,‡</sup>,  
and Rebecca Kramer-Bottiglio<sup>1</sup>

**Abstract**—Liquid crystal elastomers (LCEs) are a promising class of responsive materials for shape-morphable structures due to their large deformation, tunable properties, and low power consumption. It is well-known that by laminating a contracting LCE with an inert but flexible material layer, bending actuation can be achieved. We report a method to fabricate thermoresponsive LCE and fabric bilayer actuators and characterize their utility as bending actuators. We find that the use of different strain-limiting fabrics yields varying actuation outputs and curvatures, which we discover to be reliant on the interfacial adhesion of the bilayer, rather than the stiffness of the strain-limiting layer. We demonstrate the efficacy of the proposed LCE-fabric bending actuator in a soft robotic gripper. The findings herein can be applied to the design of LCE and fabric bilayer structure patterns to realize complex and programmable out-of-plane morphing.

## I. INTRODUCTION

Biological systems achieve controllable shape morphing in response to environmental cues that allow them to function safely and robustly in diverse environments. For example, pine cones open and close passively in response to ambient humidity [1], baobab seed pods transform from a flat sheet to a helix in response to humidity [2], and wheat awns will reversibly bend in response to their environment to propel seeds onto the ground [3]. The controlled shape morphing in these plants is due to the underlying bilayer mechanism and is critical to their growth patterns and sustenance. The bilayer mechanism is a bioinspired phenomenon of differential growth-driven morphogenesis in plants and biological tissues, wherein nonuniform growth amongst thin elastic membranes leads to out-of-plane deformations [4].

Shape morphing has been one of the primary goals in extending the vast capabilities of bioinspired soft robots [5], [6]. While systems-based actuators, such as pneumatic or hydraulic actuators, are vast and useful, stimuli-responsive materials can be used to emulate the desired bio-inspired shape-changing behavior in soft robots. Environmental cues, such as a change in temperature, humidity, or magnetic field, can warrant a response from materials that effectively pro-

<sup>1</sup>Department of Mechanical Engineering & Materials Science, Yale University, 9 Hillhouse Avenue, New Haven, CT 06520, USA. (email: rebecca.kramer@yale.edu)

<sup>†</sup>L.S.B. is currently affiliated with: Department of Radiology, Weill Cornell Medicine, New York, NY 10021, USA,

<sup>‡</sup>S.K.P. is currently affiliated with: Department of Mechanical Engineering, University of Alabama, Tuscaloosa, AL 35487, USA.

S.E. was supported by a NASA Space Technology Graduate Research Fellowship (80NSSC21K1269). L.B. was supported by a National Science Foundation (NSF) Graduate Research Fellowship (DGE-2139841). L.S.B. was supported by the NSF under grant no. IIS-1954591. S.P. was supported by the Office of Naval Research under grant no. N00014-21-1-2417.

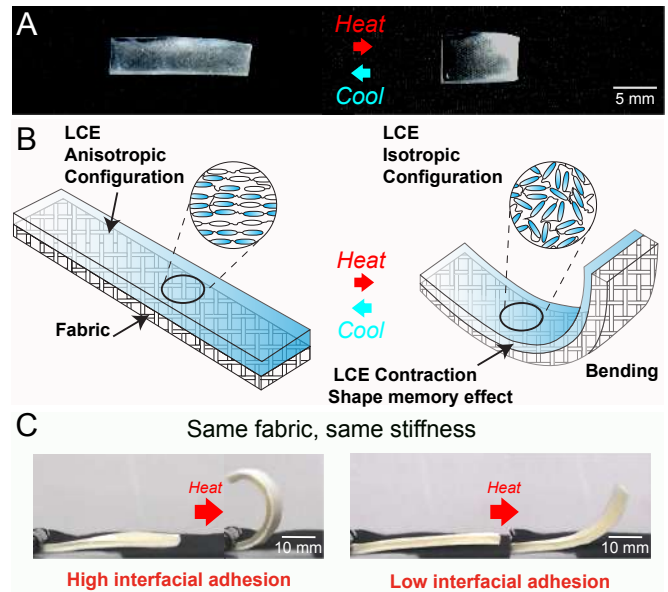


Fig. 1. A) Reversible actuation of a liquid crystal elastomer (LCE). A programmed aligned LCE (left) will contract when heated (right), and return to its initial programmed shape when cooled. B) Schematic of LCE-fabric bilayer actuators. C) Images of bilayer actuators, with high/low interfacial adhesion, undergoing curvature when subject to thermal stimuli.

vides the desired shape change. Furthermore, when stimuli-responsive materials are used in a bilayer configuration, actuation similar to natural systems can be achieved [7], [8].

In this work, we chose liquid crystal elastomers (LCEs) because of their reversible actuation and large deformation range [9], [10]. LCEs are materials that combine the long-range orientational order of liquid crystals with the entropic elasticity of traditional elastomer materials. The combination of the two counteracting properties of LCEs, ordered and disordered, results in a unique shape-memory behavior when exposed to various environmental cues. Thermotropic liquid crystals respond to a change in temperature, which has proven helpful in several applications where remote operation or tunable stimulus response is desirable [11], [12]. As a result, LCEs are an emerging technology within the soft robotic realm, attributed to their substantial thermally induced reversible shape change [10], [13].

LCEs can be programmed to hold a specific shape below their clearing temperature ( $T_c$ ; nematic state) and a separate shape past their  $T_c$  (isotropic state) (Figure 1A). Because LCEs are generally planar contracting actuators, it can be challenging to accomplish complex out-of-plane shape morphing. In previous works, out-of-plane LCE de-

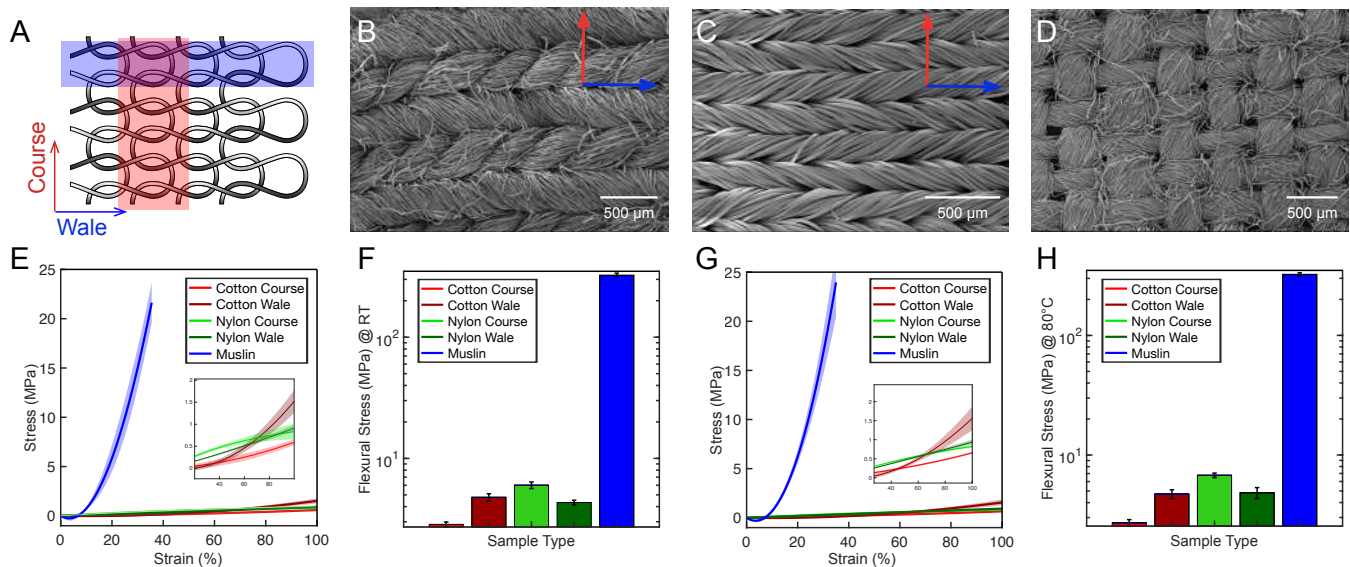


Fig. 2. A) Schematic of a knitted structure, indicating its respective components. B-D) Scanning electron microscopy (SEM) image of fabric samples of (B) cotton, (C) nylon, and (D) muslin. The colored axis represents the course and wale of relevant fabrics. E) Stress-strain measurements taken at room temperature of individual fabrics. Inset is a zoom-in of cotton and nylon samples. F) Flexural stress measurements taken at room temperature of fabric samples at 15% strain (y-axis is on a logarithmic scale). G) Stress-strain measurements taken at 80 °C of individual fabrics. Inset is a zoom-in of cotton and nylon samples. H) Flexural stress measurements taken at 80 °C of fabric samples at 15% strain (y-axis is on a logarithmic scale).

formation has been achieved with a bilayer mechanism [14], [15], but requires complex synthesis techniques for optimal interfacial adhesion. Furthermore, stretching of LCEs prior to programming has been shown to impart curvatures throughout the structure [16], [17]. Finally, modulating LCE nematic director orientations pixel-by-pixel can produce out-of-plane motion, but is time-consuming and requires solving a computationally expensive inverse design problem [18], [19], [20].

In this paper, we propose a facile fabrication procedure for shape-morphable liquid crystal elastomeric composites (SLiCEs), which are material systems that leverage the bilayer mechanism by adhering thermoresponsive LCEs to fabric strain limiters to achieve complex out-of-plane deformations (Figure 1B, Supplementary Video). We first survey and characterize several different fabrics to be used as effective strain-limiters. Thereafter, we synthesize SLiCEs and characterize their mechanical properties and actuation properties. We find that the actuation performance of the SLiCEs is dominated by the interfacial adhesion between the LCE and fabric (Figure 1C), rather than the stiffness differential between the layers. Finally, we show how the composite can be used effectively for robotic applications. With this study, we hope to provide a deeper understanding of the mechanics behind bilayer soft actuators using thermoresponsive LCEs.

## II. MATERIALS AND METHODS

*a) Synthesis of LCE:* Liquid crystal elastomer (LCE) with mesogen RM 257 was synthesized using previously described techniques [9], [21]. First, 4 g of the mesogen 1,4-Bis-[4-(3-acryloyloxypropyloxy)benzoyloxy]-2-methylbenzene (RM 257) was added to a vial with 1.6 g

of toluene and heated at 80 °C until the material became a homogeneous liquid. Thereafter, 0.217 g of pentaerythritol tetrakis(3-mercaptopropionate) (PETMP) and 0.9157 g of 2,2'-(Ethylenedioxy)diethanethiol (EDDET) were added to the solution to yield a ratio of 15:85 PETMP:EDDET. Finally, 0.0257 g (2-hydroxyethoxy)-2-methylpropiophenone (HHMP) photoinitiator and 0.568 g of diluted dipropylamine (DPA) catalyst (1:50 DPA:Toluene) were added to the solution and mixed vigorously using a Vortex mixer. The solution was poured into an acrylic mold, degassed in a vacuum to remove any bubbles, and allowed to cure overnight at room temperature. After curing, the sample was removed from the mold and placed in an oven at 80 °C overnight to remove any remaining toluene.

Programming of the anisotropic nematic state was achieved by exposing the sample to a UV light set to 365 nm wavelength for 30 min. Past the clearing temperature ( $T_c$ ), the structure will hold its isotropic as-cast state and below the  $T_c$ , the structure will hold its anisotropic nematic state.

*b) Strain-Limiting Layer:* Incorporating strain-limiting layers into the liquid crystal elastomer involves adhering pre-cut and un-stretched fabric pieces onto the LCE matrix using slightly gelled LCE. The knitted fabrics, nylon and cotton, appear to have a different front and back structure. The side of the fabric with the larger and more distinguishable topological features was chosen and consistently used throughout this study. The slightly gelled LCE was synthesized using the same chemical formula described above but was cured for approximately one minute so that the viscosity increased, enabling easier manipulation of the material to allow for attachment of the pre-cut fabric to the cured LCE samples. After that, the materials were allowed to cure under compression to yield SLiCE composites (Figure 3A).

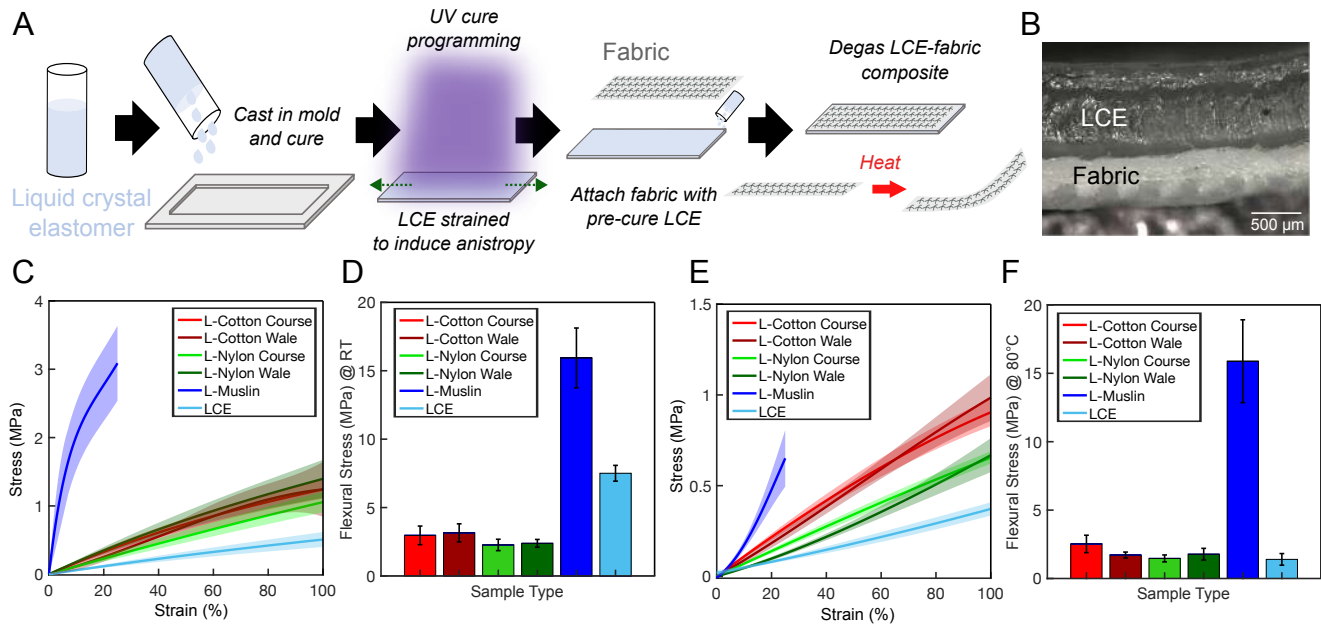


Fig. 3. A) Schematic of the synthesis method of SLiCE bilayer actuators. B) Cross-sectional optical microscopy image of a SLiCE actuator. C-F) For all SLiCE actuators and neat LCE: (C) Stress-strain measurements taken at room temperature, (D) Flexural stress measurements taken at room temperature at 50% strain. (E) Stress-strain measurements taken at 80 °C. (F) Flexural stress measurements taken at 80 °C at 50% strain.

c) *Physical and Mechanical Characterization:* Scanning electron microscopy (SEM) images were obtained using a Hitachi Su-70 at 2 kV. All samples were coated with iridium (nominally 8 nm) before SEM imaging. Cross-sectional optical microscopy images were taken with a Zeiss Smartzoom 5. Curvature measurements were filmed and post-processed using Python OpenCV image packages.

All stress-strain and 3-point bend measurements were performed using a dynamic mechanical analyzer (DMA Q850, TA Instruments). The stress-strain and 3-point bend measurements were both taken at a rate of 30 mm/min. Actuation stress and T-peel measurements were performed using a materials testing system (Instron 3345). T-peel measurements were taken at 30 mm/sec. All neat fabric samples were tested without any pre-stretching. At least five samples were tested for each mechanical characterization.

### III. FABRIC CHARACTERIZATION

Fabrics were chosen as effective strain-limiting layers to pair with LCE actuators due to our early observations of pre-cure LCE wetting, spreading, and wicking on candidate fabric substrates. Typically, fabrics are knitted or woven in a specific manner in which the fabric may have a length-wise or cross-wise grain. Figure 2A shows the directionality that may arise from knitted fabrics, which are composed of courses and wales. Figures 2B-D show scanning electron microscopy (SEM) images of the three different fabrics chosen, which are jersey cotton (knitted), nylon (knitted), and muslin cotton (woven), respectively. For the knitted patterns, jersey cotton and nylon, course and wale are indicated on the SEM images. Because muslin is a plain-weave fabric

and appears to be isotropic in the parallel and perpendicular directions, no directionality is indicated or differentiated. All knitted fabrics were mechanically characterized in either the course or wale direction (for a ‘course’ sample, the course of the fabric would be parallel to the tensile strain and perpendicular to the bending strain), and muslin is characterized in the direction parallel to the thread.

Figure 2E shows stress-strain measurements taken at room temperature for all the fabrics. Due to the high stiffness of muslin, the sample could not be strained past 25%. All of the other samples exhibit similar mechanical properties in the tensile configuration. The inset shows that in the course and wale direction, nylon typically exhibits similar properties, but there appears to be larger differences in tensile properties between cotton in the course and wale direction. Flexural stress measurements at 15% strain of the fabrics taken at room temperature show muslin having the highest flexural stress, approximately an order of magnitude higher than any of the other samples. Nylon course has a notably higher flexural stress when compared to nylon wale and cotton wale, which have similar flexural stress measurements. Cotton course does exhibit the lowest flexural stress and is therefore the least stiff in a bending configuration.

Because the fabrics will be subject to high temperatures when integrated with the LCE to enable actuation, the fabrics are tested at the  $T_c$  of LCE (80 °C). Figure 2G shows the stress-strain properties of the fabrics at the  $T_c$ . The results do not differ much from the room temperature results, where muslin is significantly stiffer than all the other fabrics. Similarly, flexural stress measurements taken at 15% strain at the  $T_c$  show that muslin has the highest

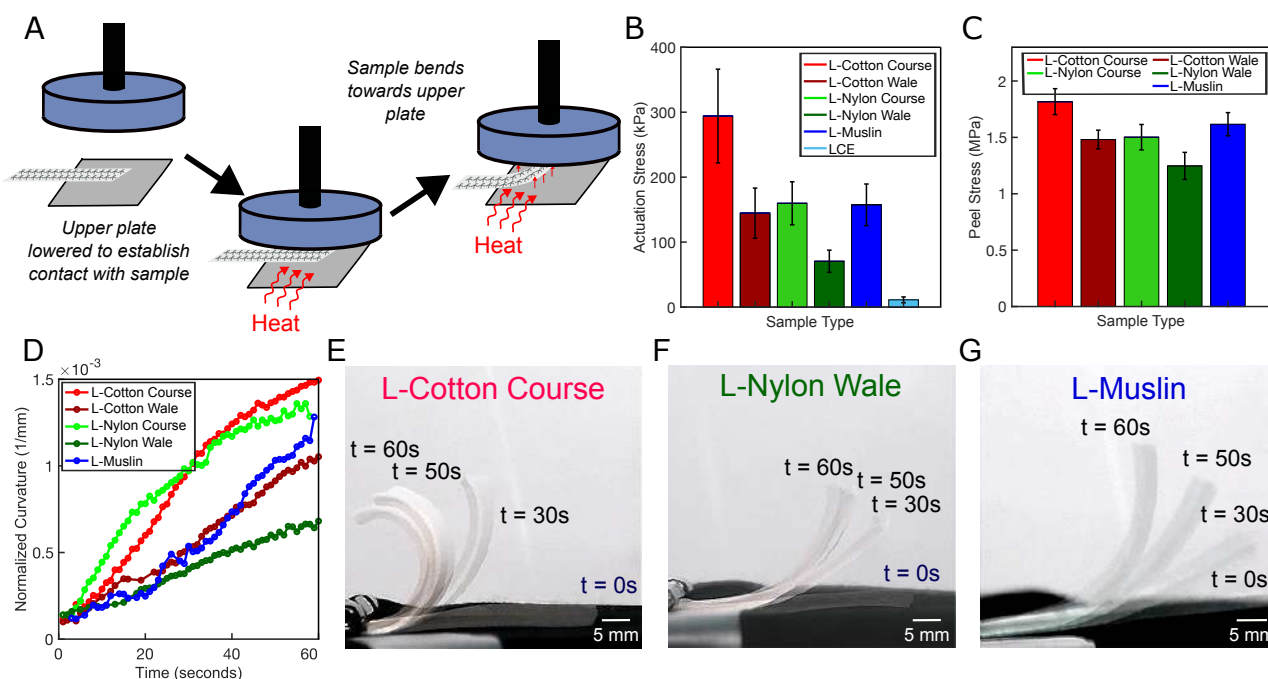


Fig. 4. A) Schematic of method to measure actuation stress of SLiCE actuators using a universal testing system. B) Actuation stress measurements of all SLiCE actuators, with neat LCE as a control. C) T-peel stress measurements of SLiCE actuators. D) Curvature measurements for each SLiCE actuator averaged over three samples. E-G) Overlaid curvature sequences of (E) cotton course composite actuator, (F) nylon wale composite actuator, and (G) muslin composite actuator over 60 seconds.

flexural stress, followed by nylon course. Nylon wale and cotton wale have similar flexural stress measurements, and cotton course exhibits the lowest flexural stiffness. Flexural stress measurements show slight variations with temperature change, unlike stress-strain measurements, which may be due to the higher strains reached in the bending configuration, corresponding to significantly higher stresses measured.

#### IV. COMPOSITE SYNTHESIS AND CHARACTERIZATION

SLiCE actuators are synthesized using the methods shown in Figure 3A. First, an LCE sample is synthesized and cured. An LCE structure can be programmed to have its mesogens in an anisotropic configuration by straining the sample under UV light. When heated past a  $T_c$  (approximately 80 °C), the LCE structure returns to its isotropic configuration by contraction. The contraction of the LCE is due to the mesogens no longer holding topological restrictions on the polymer matrix. Thereafter, the fabric is laminated to the LCE via the addition of pre-cure LCE, when the LCE is in its extended state. Post-cure, the composite is degassed, yielding a bilayered SLiCE actuator.

Due to the different directionalities of the fabric, for both cotton jersey and nylon, the fabric is attached with the wale or course pattern going along the axis of actuation on the LCE. If the wale or course is parallel to the axis of actuation, the sample is denoted as ‘wale’ or ‘course’, respectively. For the muslin samples, the fabric is attached with the thread both perpendicular and parallel to the direction of the axis of actuation. We label the composite actuators using just the fabric and directionality for simplicity, but add ‘L-’ to

distinguish composite actuators from neat fabric. Figure 3B shows a cross-sectional optical microscopy image of a SLiCE actuator.

The SLiCE actuators, which comprise both LCE and fabric, exhibit different mechanical properties compared to the neat fabrics or the neat LCE. Figure 3C shows stress-strain measurements taken at room temperature of all SLiCE composites and neat LCE. The muslin composite exhibits the highest stiffness, followed by all the other composites, with the neat LCE exhibiting the lowest stiffness values. Flexural stress measurements at 50% strain of the composites taken at room temperature show that the muslin composite exhibits the highest flexural stress, followed by neat LCE, and the other composites are all approximately within the same range of flexural stress values (Figure 3D).

When the composites are heated past the  $T_c$  of LCE, 80 °C, different trends arise in both the tensile and bending configurations. As the LCE is heated past its  $T_c$ , the LCE undergoes an anisotropic to isotropic phase-change, which reduces the overall stiffness of the LCE. The reduction in stiffness of the LCE has a noticeable effect on the SLiCE actuators, where all samples exhibited a decrease in stiffness when compared to the samples measured at room temperature (Figure 3E). However, while the muslin composite remains the stiffest at  $T_c$ , the nylon composite samples and cotton composite samples diverged from each other, showing clear distinctions in responses to tensile strain at the  $T_c$ . Flexural stress measurements at 50% strain of the composites taken at the  $T_c$  show a decrease in flexural stress for all samples except the muslin composite (Figure 3F). A

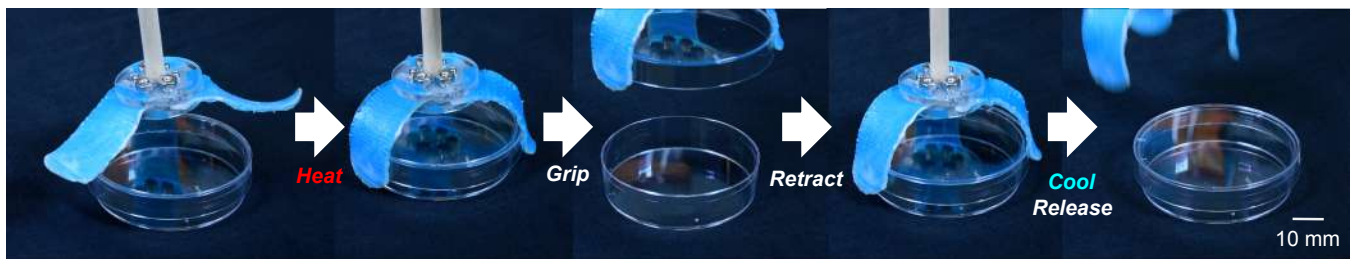


Fig. 5. Robotic gripper comprised of SLiCE actuators can grip objects when hot and release objects when cooled.

more substantial drop in flexural stress of the cotton wale composite is noted (45% reduction in flexural stress) when compared to that of the other cotton and nylon composites (approximately 20-30% reduction in flexural stress).

## V. COMPOSITE ACTUATION AND DEMONSTRATION

Due to the application of strain-limiting fabric to the LCE sample, rather than undergoing axial contraction and expansion, the actuator produces a force out-of-plane. This force can be characterized by methods shown in Figure 4A and adapted from Buckner *et al* [22], where the blocked bending tip force in response to heat is measured in a compression configuration on a universal testing system. The results of this characterization are shown in Figure 4B, where neat LCE with no strain-limiting layer is measured as a control sample. The cotton course composite exhibits the highest actuation stress value by far, with cotton wale, nylon course, and muslin composites all exhibiting approximately the same actuation stress values. Finally, the nylon wale composite exhibits the lowest actuation stress value. Interestingly, the mechanical characterizations of the composites shown in Figure 3 indicate that other than the muslin composite, the other composites all exhibit similar tensile and bending mechanical properties. However, despite having similar mechanical properties, other than muslin, the actuation properties are vastly different.

T-peel tests were conducted to determine the interfacial adhesion between the LCE and fabrics. Figure 4C shows that the measured interfacial adhesion appears to be highest for the cotton course composite, lowest for the nylon wale composite, and similar for all the remaining composites. Notably, the trends found in the T-peel measurements appear to match the trends found in the actuation stress measurements, indicating that interfacial adhesion (rather than stiffness differential) may be the dominant variable that is predictive of the actuation stress properties of LCE-fabric bilayer actuators.

Finally, the curvature of the SLiCE actuators was characterized and measured to determine if the trends with actuation stress and interfacial adhesion translated to curvature. Figure 4D shows normalized curvature with respect to time, with each line representing the average of three separate samples. While the curvature trends do follow those observed for actuation stress—with nylon wale composites exhibiting the lowest curvature, cotton wale, nylon course, and muslin composites exhibiting similar curvature paths, and finally the

cotton course composites exhibiting the highest curvature—the differences are less drastic. Figures 4E-G show overlaid curvature sequence images over 60 seconds of cotton course, nylon wale, and muslin composites respectively. The cotton course composite achieved significantly higher curvatures in the same time frame as the other two samples, with the nylon wale composite showing drastically lower achieved curvatures than the muslin and cotton course composites.

To showcase relevant demonstrations of the SLiCE actuator in the context of soft robotics, we rationally implement strain-limiting layers onto LCE to yield a three-finger robotic gripper (Figure 5). As the composite material will curl towards the direction of the contracting LCE and away from the fabric, we oriented the fabric layers to face outwards of the gripper. The LCE contracts when subject to heat, but the fabric layer acts as a strain-limiting layer, causing each bilayer to undergo a curling motion. Thereon, the gripper can grasp and lift off a petri dish lid. Once cooled, the contracted LCE layer returns to its original shape, allowing the gripper to release the item (Supplementary Video).

## VI. DISCUSSION AND CONCLUSION

In this work, we reported a simple method to laminate thermoresponsive LCE with strain-limiting fabrics to create bilayer bending actuators. The actuators, which we call SLiCE actuators, are granted actuation stress and out-of-plane curvatures. We surveyed several fabrics with different physical and mechanical properties to determine which fabric yields the most optimal actuator. In doing so, we found that the actuation stress and blocked curvature force of the bilayer actuators correspond to the interfacial adhesion between layers, as opposed to the stiffness differential between the two layers.

We elucidated how we can increase the actuation stress of bilayer actuators, which are frequently used in the field of soft robotics to enable desirable motions. For example, one might assume that because the bilayer mechanism is driven by a strain-limiting layer that prevents the actuator from contracting/extending along the plane, using the stiffest strain-limiting layer may optimize the actuation stress. However, we found that the stiffest material, muslin, does not yield the highest actuation stress. Instead, we found that the fabric that had the highest peel stress when laminated to the LCE gave the highest actuation stress, indicating the interfacial adhesion between the LCE and the fabric is

the most dominant variable that is predictive of actuation performance.

A large body of literature covering bilayer actuators indeed emphasizes interfacial adhesion. However, the motivation typically does not involve enhancing actuation stress, but rather attaching two materials that are difficult to bond together and preventing material delamination. In this study, we hope to bring attention to the important factor of interfacial adhesion, and further motivate the enhancement of interfacial adhesion between materials to optimize bilayer actuators and their actuation capabilities.

We also discovered that knitted fabrics, nylon and cotton jersey, exhibit vastly different mechanical properties when oriented in different directions, and can have varying mechanical properties at different temperatures. The orientation of the knit pattern is also very important when adhering to other substrates, as we found that when LCE is adhered parallel to the course of the fabric, the interfacial adhesion is substantially higher than when parallel to the wale of the fabric. We hypothesize the differences in adhesion may be in part due to contact splitting mechanics [23], [24]. That is, when peeling or shearing parallel to the course, the fabric presents distinct sub-contacts that would inhibit crack propagation and enhance shear adhesion. However, factors such as fiber content, knit structure, fiber morphology, and technical side adhered may also play a role in the adhesion between the fabric and the LCE. Future work will further investigate the interfacial adhesion between the fabrics and LCE, as well as the generality of our finding that bilayer actuation is more reliant on interfacial adhesion than the stiffness differential between the layers.

By using a simple method to achieve out-of-plane shape change in thermoresponsive LCEs via the addition of a strain-limiting fabric layer, and elucidating the mechanism to enhance this actuation behavior, we have contributed to the current landscape and understanding of soft bilayer actuation.

#### APPENDIX

1,4-Bis-[4-(3-acryloyloxypropoxy)benzoyloxy]-2-methylbenzene (RM 257) was purchased from Wilshire Technologies (Princeton, NJ). Toluene, Pentaerythritol tetrakis(3-mercaptopropionate) (PETMP), 2,2'-(Ethylenedioxy)diethanethiol (EDDET), Dipropylamine (DPA), and (2-hydroxyethoxy)-2-methylpropiophenone (HHMP) were purchased from Sigma Aldrich (St. Louis, MO). Nylon 4-way stretch fabric was purchased from Amazon (Rex Fabrics). Cotton jersey fabric was purchased from Amazon (Robert Kaufman). Cotton muslin fabric was purchased from Amazon.

#### REFERENCES

- [1] C. Dawson, J. F. Vincent, and A.-M. Rocca, "How pine cones open," *Nature*, vol. 390, no. 6661, pp. 668–668, 1997.
- [2] Y. Forterre and J. Dumais, "Generating helices in nature," *science*, vol. 333, no. 6050, pp. 1715–1716, 2011.
- [3] R. Elbaum, L. Zaltzman, I. Burgert, and P. Fratzl, "The role of wheat awns in the seed dispersal unit," *Science*, vol. 316, no. 5826, pp. 884–886, 2007.

- [4] E. Reyssat and L. Mahadevan, "Hygromorphs: from pine cones to biomimetic bilayers," *Journal of the Royal Society Interface*, vol. 6, no. 39, pp. 951–957, 2009.
- [5] M. Li, A. Pal, A. Aghakhani, A. Pena-Francesch, and M. Sitti, "Soft actuators for real-world applications," *Nature Reviews Materials*, vol. 7, no. 3, pp. 235–249, 2022.
- [6] N. El-Atab, R. B. Mishra, F. Al-Modaf, L. Joharji, A. A. Alsharif, H. Alamoudi, M. Diaz, N. Qaiser, and M. M. Hussain, "Soft actuators for soft robotic applications: A review," *Advanced Intelligent Systems*, vol. 2, no. 10, p. 2000128, 2020.
- [7] J. Duan, X. Liang, K. Zhu, J. Guo, and L. Zhang, "Bilayer hydrogel actuators with tight interfacial adhesion fully constructed from natural polysaccharides," *Soft Matter*, vol. 13, no. 2, pp. 345–354, 2017.
- [8] M. Rüggeberg and I. Burgert, "Bio-inspired wooden actuators for large scale applications," *PloS one*, vol. 10, no. 4, p. e0120718, 2015.
- [9] M. O. Saed, A. H. Torbati, D. P. Nair, and C. M. Yakacki, "Synthesis of Programmable Main-chain Liquid-crystalline Elastomers Using a Two-stage Thiol-acrylate Reaction," *JoVE (Journal of Visualized Experiments)*, no. 107, p. e53546, 2016.
- [10] M. J. Ford, C. P. Ambulo, T. A. Kent, E. J. Markvicka, C. Pan, J. Malen, T. H. Ware, and C. Majidi, "A multifunctional shape-morphing elastomer with liquid metal inclusions," *Proceedings of the National Academy of Sciences*, vol. 116, no. 43, pp. 21438–21444, 2019.
- [11] L. Hu, Y. Wan, Q. Zhang, and M. J. Serpe, "Harnessing the power of stimuli-responsive polymers for actuation," *Advanced Functional Materials*, vol. 30, no. 2, p. 1903471, 2020.
- [12] W. Hu, G. Z. Lum, M. Mastrangeli, and M. Sitti, "Small-scale soft-bodied robot with multimodal locomotion," *Nature*, vol. 554, no. 7690, pp. 81–85, 2018.
- [13] T. J. White and D. J. Broer, "Programmable and adaptive mechanics with liquid crystal polymer networks and elastomers," *Nature Materials*, vol. 14, no. 11, pp. 1087–1098, 2015.
- [14] A. Agrawal, T. Yun, S. L. Pesek, W. G. Chapman, and R. Verduzco, "Shape-responsive liquid crystal elastomer bilayers," *Soft Matter*, vol. 10, no. 9, pp. 1411–1415, 2014.
- [15] J. M. Boothby and T. H. Ware, "Dual-responsive, shape-switching bilayers enabled by liquid crystal elastomers," *Soft Matter*, vol. 13, no. 24, pp. 4349–4356, 2017.
- [16] Y. Li, H. Yu, K. Yu, X. Guo, and X. Wang, "Reconfigurable Three-Dimensional Mesotstructures of Spatially Programmed Liquid Crystal Elastomers and Their Ferromagnetic Composites," *Advanced Functional Materials*, vol. 31, no. 23, p. 2100338, 2021.
- [17] C. Ahn, X. Liang, and S. Cai, "Inhomogeneous stretch induced patterning of molecular orientation in liquid crystal elastomers," *Extreme Mechanics Letters*, vol. 5, pp. 30–36, 2015.
- [18] H. Aharoni, Y. Xia, X. Zhang, R. D. Kamien, and S. Yang, "Universal inverse design of surfaces with thin nematic elastomer sheets," *Proceedings of the National Academy of Sciences*, vol. 115, no. 28, pp. 7206–7211, 2018.
- [19] S. J. Abhoff, F. Lancia, S. Iamsaard, B. Matt, T. Kudernac, S. P. Fletcher, and N. Katsonis, "High-Power Actuation from Molecular Photoswitches in Enantiomerically Paired Soft Springs," *Angewandte Chemie International Edition*, vol. 56, no. 12, pp. 3261–3265, 2017.
- [20] M. E. McConney, A. Martinez, V. P. Tondiglia, K. M. Lee, D. Langley, I. I. Smalyukh, and T. J. White, "Topography from Topology: Photoinduced Surface Features Generated in Liquid Crystal Polymer Networks," *Advanced Materials*, vol. 25, no. 41, pp. 5880–5885, 2013.
- [21] C. M. Yakacki, M. Saed, D. P. Nair, T. Gong, S. M. Reed, and C. N. Bowman, "Tailorable and programmable liquid-crystalline elastomers using a two-stage thiol-acrylate reaction," *RSC Advances*, vol. 5, no. 25, pp. 18997–19001, 2015.
- [22] T. L. Buckner, R. A. Bilodeau, S. Y. Kim, and R. Kramer-Bottiglio, "Robotizing fabric by integrating functional fibers," *Proceedings of the National Academy of Sciences*, vol. 117, no. 41, pp. 25360–25369, 2020.
- [23] M. Kamperman, E. Kroner, A. Del Campo, R. M. McMeeking, and E. Arzt, "Functional adhesive surfaces with "gecko" effect: The concept of contact splitting," *Advanced Engineering Materials*, vol. 12, no. 5, pp. 335–348, 2010.
- [24] R. K. Kramer, C. Majidi, and R. J. Wood, "Shear-mode contact splitting for a microtextured elastomer film," *Advanced Materials*, vol. 22, no. 33, pp. 3700–3703, 2010.